JOURNAL OF MATERIALS SCIENCE 14 (1979) 2143–2150

Nucleation and propagation of fatigue cracks in Al–304 stainless steel laminate composite

K. K. CHAWLA
Instituto Militar de Engenharia, Centro de Pesquisa de Materiais, Pça Tiburcio, Urca, 22290 Rio de Janeiro, RJ, Brasil

P. K. LIAW
Department of Materials Science & Engineering, North Western University, Evanston, Illinois 60201, USA

A study has been made of fatigue crack nucleation and propagation in Al–stainless steel (30 vol %) laminate composites. A Paris type power relationship between the crack growth rate, da/dN, and the alternating stress intensity, ΔK, was obtained over the crack growth rates ranging from 10^{-7} to 10^{-4} mm/cycle, with an exponent m of 2.7. The cracks nucleated first in Al strips and then in stainless steel strips accompanied by some interface decohesion. The fatigue crack propagated in two stages. In the first stage, where the Al–steel interface was largely intact, the crack propagated in a plane strain mode (flat fracture surface with striations, each striation consisting of a cluster of interstriations). In the second stage, where there occurred extensive Al–steel interface delamination and the concomitant loss of mutual constraint, the crack propagated in the plane stress mode (slant fracture with voids). The crack growth was faster in Al than that in steel since the apparent striation spacing was larger in the former than in the latter. No one to one correspondence existed between the apparent striation spacing and the macroscopic crack growth rate.

Thus, although, microscopically, the crack front was not planar; macroscopically, it could be regarded as planar, and a Paris type power relationship did characterize the macroscopic fatigue crack growth in this laminate system over the applied stress amplitude studied. Comparing the fatigue crack growth rates among Al–steel laminate, commercial or pure aluminium and 304 stainless steel, the Al–steel laminate has the lowest crack growth rate. This plus the weight and cost saving benefits make Al–steel laminate quite attractive.

1. Introduction

Laminate reinforcement offers a definite advantage over fibrous reinforcement in that the former is bidimensional (planar) while the latter is unidirectional. Despite the fact that laminates are used, in one form or another, in electrical, electronic, chemical and mechanical industries, there exists a dearth of scientific studies of such materials. For example, in a recent review by Wright and Levitt [1] of "... the broad and rapidly growing field of metal laminates", there is not even a mention of fatigue properties of metal laminates. The present study was undertaken to examine the fatigue behaviour of the laminate system consisting of commercial purity aluminium and stainless steel 304. Specifically, it was intended to study the fatigue crack nucleation site(s) and the modes of propagation of such nucleated cracks in the two components of the composite system. An important question concerns the shape of the crack front in such composites, as these consist of materials with quite dissimilar properties. Some doubts have been expressed about the validity of applying the con-

0022–2461/79/092143–08 $02.80/0

ventional linear elastic fracture mechanics to such composites [2], mainly because of the lack of normal orientation of the crack front to the applied stress, and a non-collinear crack growth, i.e., the direction of crack growth in a composite will be influenced by the presence of weak planes, e.g., in the present case such planes of weakness will be the interfaces between Al and stainless steel.

2. Experimental methods

The fabrication and the mechanical properties of Al–304 stainless steel laminate composites have been reported elsewhere [3]. Suffice here to mention that the laminates were fabricated by hot roll bonding at about 600 K without forming any adverse reaction products at the interface. The specimens used had 30 vol% stainless steel and the monotonic yield stress was 250 MPa. The stainless steel and Al lamina were about 0.3 mm and 1 mm thick, respectively.

The fatigue crack nucleation and propagation was studied using an MTS closed loop electro-hydraulic testing machine of 90 kN capacity. All tests were conducted at room temperature and in air. The tests were conducted under stress control using a sinusoidal wave form with an R ratio ($\sigma_{min}/\sigma_{max}$) of 0.05 and a frequency of 30 Hz in pull-pull. The alternating stress intensity factor was determined by using the expression.

$$\Delta K = \Delta\sigma\sqrt{a_i} f(a_i \times w)$$

where $\Delta\sigma$ is the nominal cyclic stress amplitude, a_i is the crack length corresponding to the i value of crack velocity and $f(a_i \times w)$ is the Pook correction factor, [4] for a single edge notched specimen with a finite width, and is given by

$$f(a_i \times w) = 5\sqrt{\pi}\left[20 - 13\left(\frac{a_i}{w}\right) - 7\left(\frac{a_i}{w}\right)^2\right]^{-1/2}$$

where w is the width of the specimen. The stress concentrating notch for inititating the fatigue crack was a side notch normal to the stress axis, cut by a wire saw. The geometry of the notch, due to Kung [5], is shown in Fig. 1. The notch geometry should satisfy the following requirements [5]: (i) the notch depth should be within the focal distance of the microscope; (ii) the notch depth and radius should provide a large enough stress concentration to facilitate microcrack initiation; (iii) the notch base should be large enough to prevent any effect of the notch curvature on the microstructure of the material; (iv) the notch should be easily polishable and reproducible. The wire used to make the notch was a Cu–Be alloy (radius 0.19 mm) which ran through an abrasive slurry consisting of 9.5 μm alumina suspended in a light water soluble oil. Then 6 μm and 1 μm diamond pastes were used for mechanical polishing. This procedure gave a reasonably polished notch surface. The Inglis stress concentration factor, K_t, was 5.26. ($K_t = 1 + 2\sqrt{(a_0/\rho)}$ where a_0 is notch depth and ρ is notch radius.)

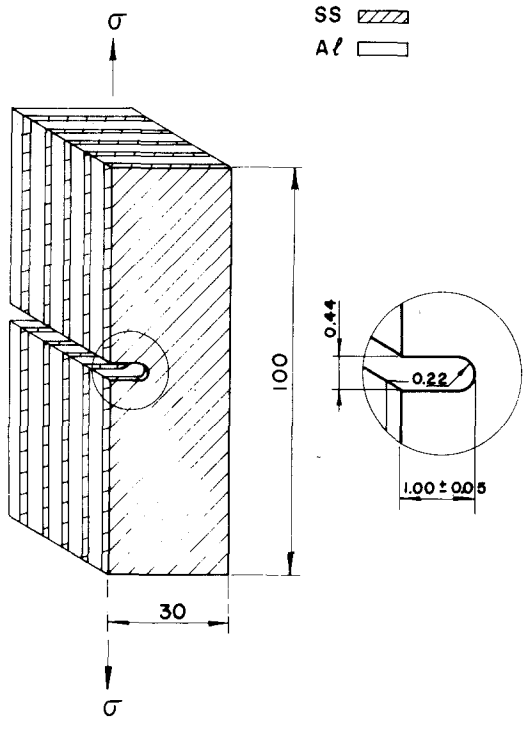

Figure 1 The notch geometry. All dimensions are in mm.

A 400 × optical microscope with a long distance focal length objective was used to monitor the crack nucleation at the notch base. The crack length measurements were made using a travelling microscope with a readable accuracy of 2 μm. Crack velocity was determined by fitting least square method to three consecutive sets of points on a fatigue crack, a, versus number of stress cycles, N, plot. Crack velocity, da/dN, was then taken as the slope of the cyclic curve at the central point.

In two samples, fatigue initiation testing was interrupted after 450 000 (high applied amplitude, $\sigma_{max} = 206.7$ MPa, $\sigma_{min} = 10.3$ MPa) and 700 000

cycles (low applied stress amplitude, σ_{max} = 87 MPa, σ_{min} = 4.4 MPa) and the notch bases were examined in SEM for studying crack nucleation. As it was difficult to obtain a smooth polish in the notch, mainly because of the different abrasion and electrolytic properties of Al and strainless steel, these samples were etched lightly with Villela's reagent, before examining in SEM, in order to facilitate observation of cracks. One sample was fatigued until fracture and the fracture surfaces were examined in SEM for observing the modes of crack propagation. Fatigue crack propagation results were obtained from this sample.

3. Results

We shall present the results in two parts. In the first part are presented the fatigue crack propagation rate results as per Paris-type relation [6], treating the composite as a monolithic material, i.e., ignoring the basic fact of its heterogeneity in structure. In the second part we present the results of microstructural examination with regard to the nucleation and propagation of fatigue cracks, taking due account of the heterogeneity of the microstructure. Finally, we discuss the results of the first part in light of the microstructural observations of the second part.

3.1. Fatigue crack propagation rate

The Paris relation, $da/dN = C(\Delta K)^m$, where C is a material constant and m is the exponent, has been found to describe reasonably well the fatigue crack growth for many monolithic metals [6]. Its application to a laminate composite is not straightforward. The fatigue behaviour of such a composite will depend on the amount and properties of each component as well as the resistance of the interfacial bond. The fatigue crack growth rate as a function of the alternating stress intensity factor, ΔK, is shown in Fig. 2. The Paris relation, using a least square analysis, takes the form

$$(da/dN) = 2.13 \times 10^{-8} (\Delta K)^{2.69}$$

where (da/dN) is in mm/cycle while ΔK has the units of MPa$\sqrt{m}$. From literature [7–9] we find that the values of m for 304 stainless steel and commercially pure aluminium are 3.1 (or 3.25) and 2.9, respectively. The value of 2.69 for m in the case of the present laminate seems to be in the same range. A value between 2 and 3 of the exponent m in the linear region of log da/dN versus log ΔK is not uncommon [10, 11]. And in view of the fact that the m value of Al and 304 stainless steel are not very different when tested alone, one would not expect a very different value when the two components are tested in the form of a composite. Thus, this kind of fracture mechanics analysis serves to characterize the fatigue crack growth in this composite. In other words, for macroscopic characterization purpose one may regard this Al–stainless steel composite laminate as a monolithic homogeneous material.

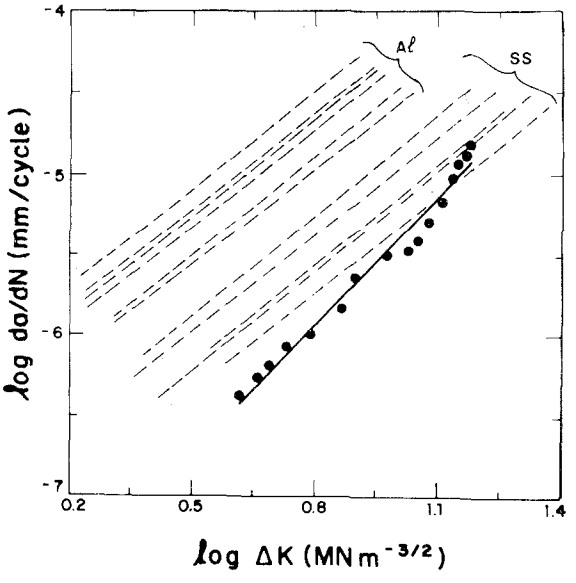

Figure 2 Fatigue crack growth rate, da/dN, as a function of the cyclic stress intensity factor, ΔK. Dashed lines are from [8, 15, 17]. Solid line and data points are for Al–SS laminate of this work.

3.2. Nucleation of fatigue cracks

From the optical microscopic observations made during the fatigue test, the following facts emerged regarding the nucleation of cracks. For cycling between a maximum nominal stress of 206.7 MPa and a minimum stress of 10.3 MPa (the high applied stress amplitude test) at 30 Hz, the first cracks appeared in Al strips between 175 000 and 200 000 cycles. By 225 000 cycles one could observe cracks in all the aluminium strips while by 350 000 cycles one crack had propagated in a stainless steel strip. The microstructural situation at 450 000 cycles, when the test was terminated and the specimen was examined in SEM, is shown in the SEM micrographs of the etched samples, Fig. 3. Fig. 3a shows that there are a number of zig-zagging cracks in the Al strip (marked by thin

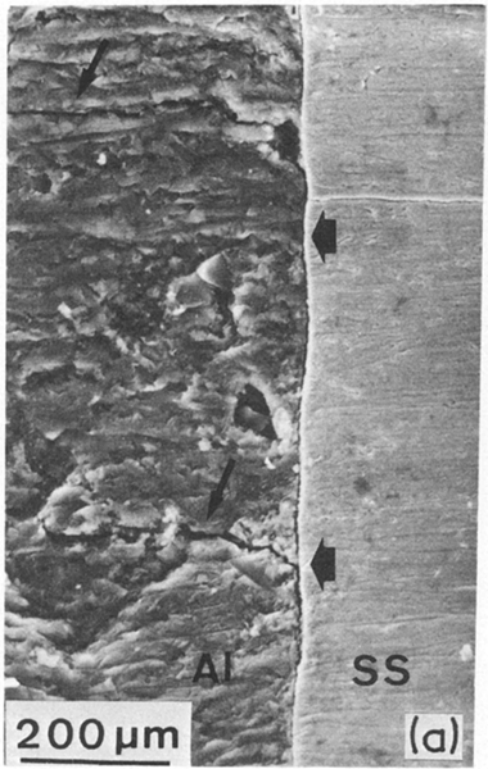

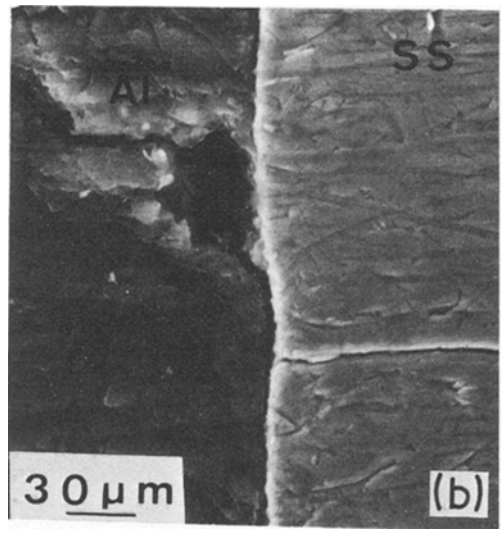

Figure 3 (a) Zig-zagging cracks in Al (thin arrows) and interface delamination (thick arrows). (b) Crack in Al strip propagates into steel strip after getting deflected at the interface.

arrows). Delamination has occurred along the interface Al–stainless steel (indicated by thick arrows). At one place, the crack in Al, after having deflected along the interface, has propagated into the steel strip. This is shown more clearly in Fig. 3b. The cracks in Al probably nucleated at some inclusions, as shown in Fig. 4, and not necessarily at the centre of the notch base where the stress concentration is most severe. On the other hand, in steel, the crack did not initiate at inclusions but, more or less, at the notch base centre where the stress concentration is the highest. Virtually the same sequence of crack nucleation was observed in the other sample cycled between 87 MPa and 4.4 MPa (the low applied stress amplitude test) and the end of the nucleation stage (i.e., as the fatigue cracks linked one another and grew across the whole notch base) in this test came at about 700 000 cycles. The total picture of the fatigue nucleation at low and high applied stress amplitudes is shown in Fig. 5. The applied stress amplitude did not affect the mode of fatigue initiation in this laminate composite system.

3.3. Crack propagation

Both aluminium and stainless steel showed two regions of crack propagation: a plane strain (90° to the stress axis), more or less flat region in the initial part of crack propagation and a plane stress (~ 45° to the stress axis), slant fracture in the latter part of crack propagation. The former (more or less flat fracture) is shown in Fig. 6. The transition to the slant fracture and slant fracture are shown in Fig. 7. If aluminium and stainless steel

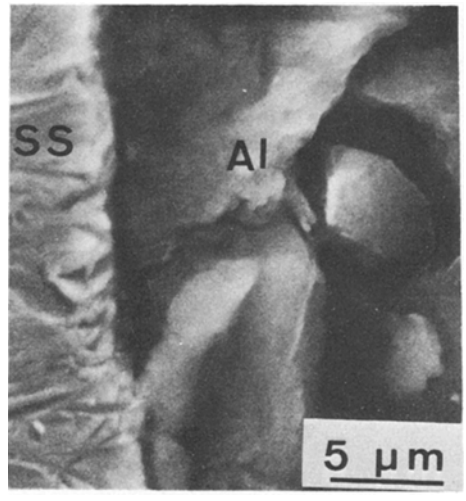

Figure 4 Crack nucleation at an inclusion in Al.

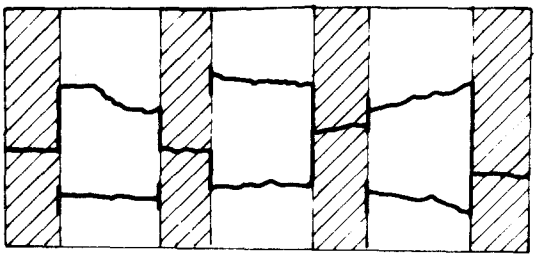

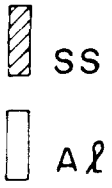

Figure 5 Schematic drawing of the situation at the end of crack nucleation.

sheets (thickness less than 1 mm) were tested individually, they would probably show a 100% slant fracture characteristic of thin sheets. In such thin sheets, the stress in the thickness direction is negligible and the stress state is one of plane stress. However, when one makes a composite of these sheets, then, so long as the adhesion between the sheets is maintained, the surfaces of sheets cannot be regarded as free surfaces. Thus, we observe relatively flat fractures in both Al and stainless steel in the initial part of fatigue crack propagation, i.e., the two components deform as if they were the central region of a relatively thick sample and under plane strain conditions (Fig. 6). The initial fracture is a mixture of slant and flat in aluminium, while that in steel is flat. With the occurrence of some interface decohesion during the fatigue test, the mutual constraint on the sheets is gradually lost with the result that they start behaving more or less like samples of thickness intermediate between that of plane strain and that of plane stress. Accordingly, we observe a transition in the fracture mode from a predominatly flat one to a predominantly slant one (Fig. 7). Microstructural examination in SEM also showed that in the flat portion of fracture the adhesion between the sheets of Al and stainless steel was more or less maintained (Fig. 6) while in the region suffering extensive delaminations there occurred out of plane deformations involved in the mode III propagation. The two components, at this point, tend to behave as if devoid of any mutual constraint.

The SEM observations of fracture surfaces showed the presence of fatigue striations in both Al and stainless steel in the plane strain, i.e., flat, fracture region. These features are shown in Fig. 8 a to c. Fig. 8a shows interface decohesion also, while Figs. 8b and c show striations at a higher magnification in Al and stainless steel, respectively. In Fig. 8b one notes that what appears to be a single striation at low magnification (Fig. 8a), in fact, consists of a cluster of interstriations. Laird *et al.* [12, 13] also found this phenomenon in cold rolled copper. The formation of interstriations were attributed by them to the rubbing together of the fracture surfaces or to the plastic blunting process. Thus, these interstriations represented only local fatigue crack growth rate and no one to

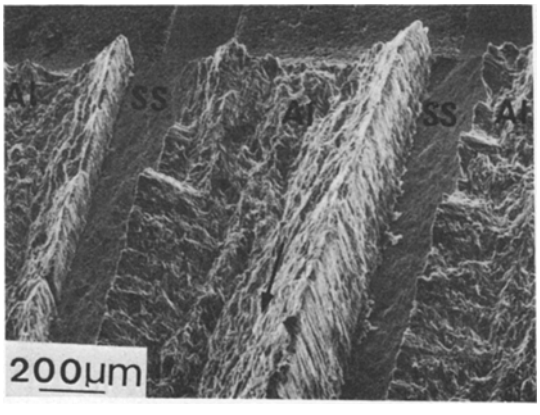

Figure 6 Plane strain (more or less flat) fracture.

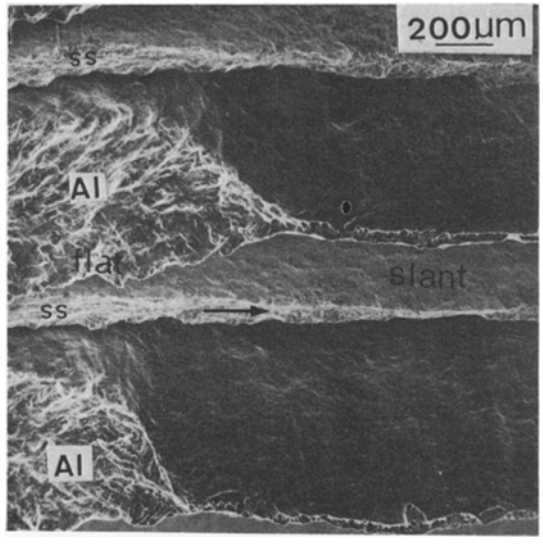

Figure 7 Transition to plane stress and plane stress (slant) fracture.

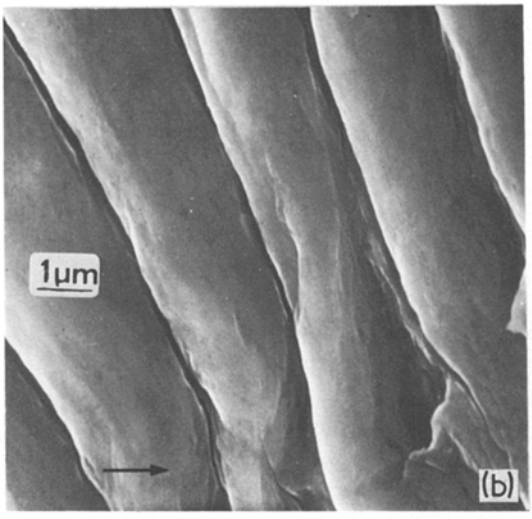

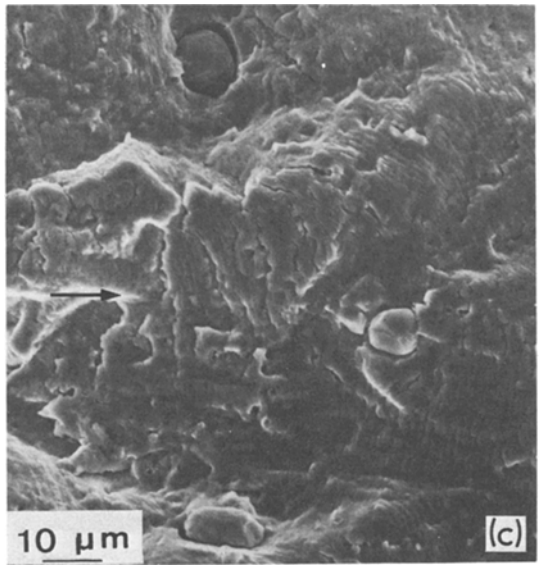

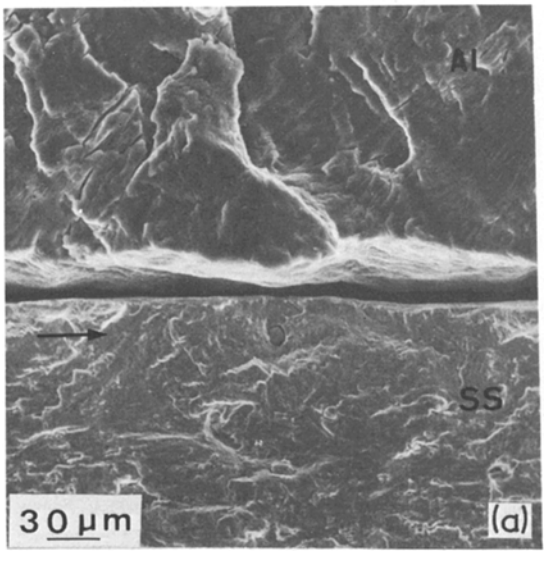

Figure 8 (a) Fatigue striations in the plane strain (flat fracture) region. Also notice the interface decohesion. (b) and (c) striations in Al and steel, respectively, at higher magnifications. Notice that the apparent striation spacing is greater in Al than that in steel and that what appears as a single striation consists, in fact, of some interstriations. The arrow indicates the crack growth direction.

one correspondence between the macroscopic and the microscopic crack growth rates was observed. On the other hand, the apparent striation spacing increased in both Al and stainless steel as the fatigue crack grew. The increase was more marked in Al than in steel. Fig. 9 shows this in Al. This implies that the rate of crack growth in both the components increased with increasing ΔK. In Fig. 8c one sees big inclusions and it is known [14] that voids form at inclusions ahead of crack and that fatigue cracks jump over the inclusions i.e., there are bursts of high growth rates around inclusions. The total fatigue crack growth rate, thus, is the sum of two parts: (i) slow crack growth rate in matrix, and (ii) fast crack growth at inclusions. A small amount of brittle inclusions is more effective in increasing the fatigue crack growth rate than a large quantity of ductile second phase [14]. An energy dispersive analysis showed that these big inclusions in stainless steel, invariably, contained Ti and most probably consisted of carbides of Ti. This is not surprising as Ti is used to stabilize carbides in the production of stainless steel.

Along with the transition in the fracture mode pointed out above (from flat to slant), there occurred a transition from striations to a void structure in both Al and stainless steel. The same results have been found in aluminium of 99.99$^+$ purity [15]. Beyond the striations, i.e., beyond the transition region, one observed a large quantity of elongated voids perpendicular to the crack growth direction (similar to the static ductile fracture), Fig. 10.

4. General discussion

Kula *et al.* [16] studied fatigue crack growth in a two layer roll boned steel laminate consisting of a high carbon layer and a low carbon layer. They found that the fatigue crack growth rate was higher in the high carbon layer than that in the low carbon layer. They did not observe decohesion

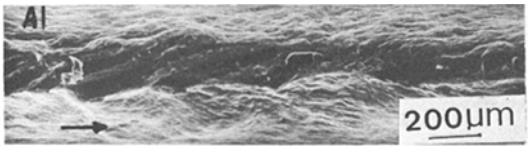

Figure 9 Increasing apparent striation spacing in Al with increasing crack length. The arrow indicates the crack growth direction.

at the interface, i.e., the crack front remained continuous, although, it was not always normal to the stress axis. Kula *et al.* pointed out the non-availability of analytical expressions for K for such kinds of crack fronts. The situation seems to be even more complex in our case. From the observations on fatigue crack nucleation and propagation in Al–stainless steel laminates, one sees that the cracks invariably nucleated in aluminium sheets first and then stainless steel strips. Also, there occurred some delamination during nucleation and the initial stages of propagation, and extensive interface delamination during the second half of crack propagation. Thus, unlike in the steel laminate of Kula *et al.*, the crack front in those Al–stainless steel laminates was, microscopically, certainly not planar. The crack did follow planes of weakness, as expected. But, macroscopically, the crack grew essentially normal to the applied stress direction. This was reflected in observance of a Paris type power law between the crack propagation rate and ΔK.

It is of interest to compare the fatigue crack propagation rates in commercial or pure Al, in 304 stainless steel and in the laminate Al–SS. The fatigue crack propagation results for commercially pure Al and 304 stainless steel, obtained from [8, 15, 17] are plotted in Fig. 2 together with that of the laminate Al–SS. One notes that the laminate Al–SS has much lower fatigue crack propagation rate than Al. The fatigue crack growth rate for the laminate Al–SS is located at the lower side of the scatter hand of 304 stainless steel. This is of great significance in as much as the laminate Al–SS has the advantages of being lighter and cheaper than stainless steel.

4. Conclusions

(1) A Paris-type power relationship between da/dN and ΔK was obtained for Al–304 stainless steel laminate composites over crack growth rates ranging from 10^{-7} to 10^{-4} mm/cycle with an exponent m of 2.69 which is close to the individual value of Al or 304 stainless steel.

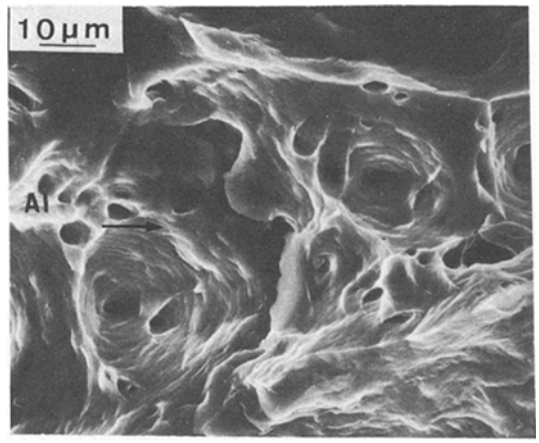

Figure 10 Transition from striations to void fracture in Al.

(2) The cracks invariably nucleated first in Al strips and then in stainless strips with some interface decohesion. This mode of fatigue crack initiation was the same over the range of applied stress amplitude.

(3) The crack propagation occurred in two parts. In the initial part, where the Al–steel interface was intact, the crack propagated in the plane strain mode and the fracture observed was flat and showed fatigue striations. Each striation consisted of a cluster of interstriations.

In the second part, where there occurred extensive Al–stainless steel interface separation and thus loss of mutual constraint, the crack propagated in the two components in the plane stress mode and a slant fracture was observed. The fatigue crack grew faster in Al since the apparent striation spacing in Al was larger than that in steel. However, the striation mechanism of crack growth was a local phenomenon and no one to one correspondence existed between the striation spacing and the macroscopic crack growth rate.

(4) Although, microscopically, the crack front was not planar, macroscopically, it could be regarded as planar. Thus, the power relationship between da/dN and ΔK did indeed characterize the macroscopic fatigue crack growth in these Al–stainless steel composite laminates over the applied stress amplitude studied.

(5) The fatigue crack propagation rates in Al–304 stainless steel laminate were located on the lower side of the scatter band of 304 stainless steel and were much smaller than that of Al (pure or commercial). This coupled with the weight and cost savings of replacing stainless steel 304 makes the laminate composite quite promising.

Acknowledgements

This work was supported in part by Organization of the American States and FINEP, CNPq through IME Materials Research Centre. Part of the experimental work was done at Northwestern University where K. K. Chawla was a Visiting Scholar through an OAS grant.

The use of the Central Facilities of Northwestern University of Materials Research centre (NSF-MRL grant DMR 76-80847) facilitated this work. The authors are extremely grateful to Dean M. E. Fine for his constant encouragement and helpful discussions of the work. Thanks are due to Professor J. D. Embury for a critical reading of the manuscript and suggestions.

References

1. E. S. WRIGHT and A. P. LEVITT, in "Metallic Matrix Composite", K. G. Kreider (ed.) vol. 4, in the series "Composite Materials" (Academic Press, New York, 1974) p. 37.
2. B. W. ROSEN, Proceedings 1975 International Conference on Composite Materials, vol. 1, TMS-AIME, New York, (1976) p. 669.
3. K. K. CHAWLA and C. E. COLLARES, Proceedings 1978 International Conference on Composite Materials, TMS-AIME, New York, (1978) p. 1237.
4. L. P. POOK, *Int. J. Fract. Mech.* 4 (1968) 295.
5. C. Y. KUNG, Ph.D. Thesis, Northwestern University, (1978).
6. P. C. PARIS and F. ERDOGAN, *J. Basic Eng.* 85 (1963) 528.
7. N. W. FROST, L. P. POOK and K. DENTON, *Eng. Fract. Mech.* 3, (1971) 109.
8. S. T. ROLFE and J. M. BARSOM, "Fracture and fatigue control in structures" (Prentice-Hall, New Jersey, 1977) p. 240-241.
9. N. E. FROST, K. J. MARSH and L. P. POOK, "Metal Fatigue" (Clarendon Press, Oxford, 1974) p. 249.
10. R. P. RITCHIE and J. F. KNOTT, *Acta Met.* **21** (1973) 639.
11. C. E. RICHARDS and T. C. LINDLEY, *Eng. Fract. Mech.* 4 (1972) 951.
12. C. LAIRD, in "Fatigue crack propagation" (ASTM STP 415, ASTM, Philadelphia, 1967) p. 131.
13. R. C. BOETTNER, C. LAIRD and A. J. MCEVILY, *Trans. TMS-AIME,* 233 (1965) 379.
14. R. M. N. PELLOUX, *Trans. ASM* 57 (1964) 511.
15. LORI TERRIEN, P. K. LIAW and M. E. FINE, unpublished data (1978).
16. E. B. KULA, A. A. ANCTIL and H. A. JOHNSON, in "Fatigue of Composite Materials" (ASTM STP 569, ASTM, Philadelphia, 1975) p. 53.
17. N. E. FROST, *J. Mech. Eng. Sci.* **1** (1959) 151.

Received 27 November 1978 and accepted 6 February 1979